

# Toward In-Field Determination of Nitrate Concentrations Via Diffusive Gradients in Thin Films—Incorporation of Reductants and Color Reagents

Thomas D. W. Corbett,\* Adam Hartland, William Henderson, Gerald J. Rys, and Louis A. Schipper



Cite This: *ACS Omega* 2022, 7, 10864–10876



Read Online

ACCESS |



Metrics & More

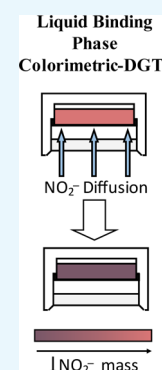


Article Recommendations



Supporting Information

**ABSTRACT:** Diffusive gradients in thin films (DGTs) have been established as useful tools for the determination of nitrate, phosphate, trace metals, and organic concentrations. General use of DGTs, however, is limited by the subsequent requirement for laboratory analysis. To increase the uptake of DGT as a tool for routine monitoring by nonspecialists, not researchers alone, methods for in-field analysis are required. Incorporation of color reagents into the binding layer, or as the binding layer, could enable the easy and accurate determination of analyte concentrations in-field. Here, we sought to develop a chitosan-stabilized silver nanoparticle (AuNP) suspension liquid-binding layer which developed color on exposure to nitrite, combined with an Fe(0)-impregnated poly-2-acrylamido-2-methyl-1-propanesulfonic acid/acrylamide copolymer hydrogel [Fe(0)-p(AMPS/AMA)] for the reduction of nitrate. The AuNP-chitosan suspension was housed in a 3D designed and printed DGT base, with a volume of 2 mL, for use with the standard DGT solution probe caps. A dialysis membrane with a molecular weight cutoff of <math><15\text{ kDa}</math> was used, as part of the material diffusion layer, to ensure that the AuNP-chitosan did not diffuse through to the bulk solution. This synthesized AuNP-chitosan provided quantitative nitrite concentrations (0 to 1000 mg L<sup>-1</sup>) and masses (145 μg) in laboratory-based color development studies. An Fe(III)-impregnated poly-2-acrylamido-2-methyl-1-propanesulfonic acid/acrylamide copolymer hydrogel [Fe(III)-p(AMPS/AMA)] was developed (10% AMPS, and 90% AMA), which was treated with NaBH<sub>4</sub> to form an Fe(0)-p(AMPS/AMA) hydrogel. The Fe(0)-p(AMPS/AMA) hydrogel quantitatively reduced nitrate to nitrite. The total nitrite mass produced was ~110 μg, from nitrate. The diffusional characteristics of nitrite and nitrate through the Fe(III)-p(AMPS/AMA) and dialysis membrane were 1.40 × 10<sup>-5</sup> and 1.40 × 10<sup>-5</sup> and 5.05 × 10<sup>-6</sup> and 5.15 × 10<sup>-6</sup> cm<sup>2</sup> s<sup>-1</sup> at 25 °C respectively. The Fe(0)-hydrogel and AuNP-chitosan suspension operated successfully in laboratory tests individually; however, the combined AuNP-chitosan suspension and Fe(0)-hydrogel DGT did not provide quantitative nitrate concentrations. Further research is required to improve the reaction rate of the AuNP-chitosan nitrite-binding layer, to meet the requirement of rapid binding to operate as a DGT.



## 1. INTRODUCTION

The increase in nitrate concentrations in freshwater systems is in part a result of the increased application of nitrogen fertilizers and cultivation of nitrogen fixers in food production and cropping. Discharge of wastewater into the environment has also led to increased environmental concentrations. Importantly, a single nitrogen atom can impact all biospheres before denitrification back to N<sub>2</sub>, as it is sequentially transferred from agricultural land, through freshwater systems to the ocean.<sup>1</sup> Measurement and determination of nitrate concentrations are therefore paramount to understand and reverse the negative effects associated with increased nitrate inputs into nutrient-sensitive ecosystems.

Numerous techniques have been deployed for the measurement and determination of nitrate concentration, each having advantages and disadvantages. Grab sampling and the determination via colorimetry, ion chromatography, or electrochemistry are the most common methods.<sup>2,3</sup> Determination via colorimetry is a two-step process. Nitrate is reduced to nitrite which produces a measurable color change when further reacted with Griess reagents or one of the many

modifications.<sup>4</sup> While grab sampling is simple and cheap, the temporal variability of nitrate concentrations is difficult to account for via grab sampling.<sup>5</sup> Samples require chemical or physical preservation, due to the potential microbial and chemical transformations nitrate can undergo during transport and storage.<sup>5</sup> Continuous sampling methods more effectively capture the temporal variability of nitrate.<sup>6</sup> They require, however, investment in expensive onsite equipment.

The in-field determination of nitrate via the automated multiplexed pumping system and UV–vis field spectrophotometer-coupled system<sup>7</sup> overcomes transport and storage restrictions. The automated multiplexed pumping systems and UV–vis field spectrophotometer-coupled systems, however, are expensive and require careful calibration via grab

Received: November 2, 2021

Accepted: March 3, 2022

Published: March 21, 2022



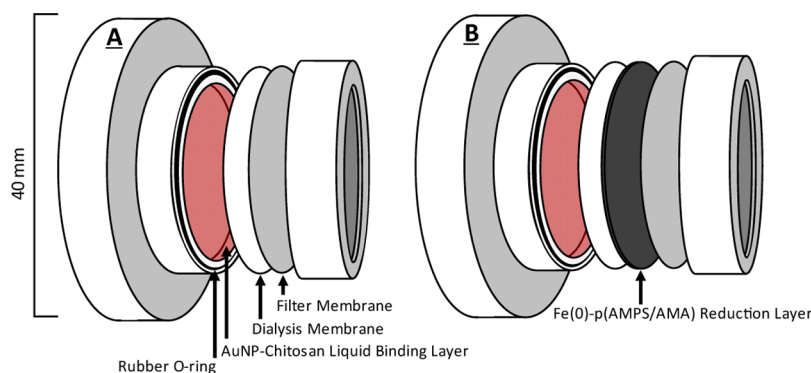


**Figure 1.** (A) Liquid-binding phase DGT solution probe (volume = 2 mL) with 1.5 mL of AuNP-chitosan suspension. A hydrogel-binding layer (A520E) and diffusive layer replace the liquid-binding layer/O-ring and dialysis membrane, respectively, in the standard nitrate DGT. (B) Combined Fe(0) reducing hydrogel and AuNP-chitosan liquid-binding layer DGT solution probe.

sampling.<sup>7</sup> They are also limited by data storage, cuvette fouling, and battery power.<sup>7</sup>

Diffusive gradients in thin films (DGTs), **Figure 1**, can overcome many of the challenges described above. DGT is a passive sampling system which provides time-weighted average concentration based on Fick's first law of diffusion<sup>8</sup> due to their random heat motion, molecules and ions move from areas of high concentration as to make the concentration uniform.<sup>9</sup> The binding layer rapidly and strongly binds a selective analyte, ensuring that the concentration is effectively zero at the binding layer/diffusive layer interface, maintaining the concentration gradient through the hydrogel diffusive layer and filter membrane.<sup>8,10</sup> This enables the calculation of the average concentration upon measuring the bound mass.<sup>8,10</sup>

DGTs make use of hydrogels to both hold analyte-selective resins and constrain transport of ions to the binding layer to diffusion. Hydrogels are polymeric materials with hydrophilic structures which enable them to retain large quantities of water within their three-dimensional network.<sup>11</sup> Investigations into alternative DGT-binding phases have explored the use of liquid-binding phases<sup>12</sup> (**Figure 1**), similar to the setup utilized by pore water equilibrators (peepers).<sup>13</sup> The liquid-binding phase DGT often makes use of commercially available dialysis membranes with tunable molecular weight cutoffs and high-molecular-mass soluble polymers.<sup>12,14</sup> An Fe<sub>3</sub>O<sub>4</sub> nanoparticulate aqueous suspension has been developed for the measurement of arsenic.<sup>14</sup>

DGTs require laboratory analysis of the mass bound to the binding layer, although DGT do not require immediate analysis, unlike grab samples. Incorporation of a color change mechanism that occurs in situ within the binding layer could overcome the necessity for laboratory analysis. It requires, however, the incorporation of reducing agents into the diffusive layer, to reduce nitrate to nitrite, prior to the color change reaction in the binding layer whether it is a liquid or a hydrogel.

Numerous gold and silver nanoparticles (AuNPs) have been reported, with varying degrees of selectivity for nitrite.<sup>15–17</sup> Gold nanoparticles have numerous properties which make their use advantageous over other metal nanoparticles for the colorimetric determination of nitrite, such as their distance-dependent optical properties,<sup>18</sup> well-defined color change,<sup>19</sup> and high stability.<sup>20</sup> For example, a chitosan-stabilized gold nanoparticle decorated reduced graphene oxide, for the selective and sensitive detection of nitrite.<sup>17</sup> Aggregation of the chitosan-stabilized gold nanoparticles, arising from their

closer formation, produced a wine red to purple color change.<sup>17</sup>

The objective of this study was to develop and establish a nitrate DGT solution probe that produced a color change within the binding layer, for the colorimetric determination of nitrate. To achieve this, this research addressed the following: (i) the establishment of a straightforward method for the preparation of zero-valent metal-impregnated hydrogel sheets for nitrate reduction to nitrite in the diffusive layer and (ii) the incorporation of a nanoparticle into the binding layer that provided a quantitative color change in the presence of nitrite.

## 2. METHODS AND MATERIALS

The development of the AuNP color reagents for use as a binding layer in DGT necessitated the development of a nitrate-reducing hydrogel. The following section details the methods used in this study to produce an Fe(0)-impregnated hydrogel for the reduction of nitrate to nitrite, and the AuNP-chitosan-binding layer for colorimetric determination of nitrite.

**2.1. General Procedures.** All reagents were sourced from Merck, New Zealand, unless otherwise stated. DGT bases and caps were sourced from DGT Research (Lancaster, United Kingdom). All solutions were prepared utilizing 18.2 MΩ deionized water. All labware were cleaned with 10% HCl for 24 h, before being thoroughly rinsed with deionized water (18.2 MΩ).

Poly(acrylamide-2-acrylamido-2-methyl-1-propanesulfonic acid) (p(AMA/AMPS)) copolymer hydrogels were prepared using 99% pure 2-acrylamido-2-methyl-1-propanesulfonic acid, 40% acrylamide, and 99% *N,N'*-methylenebisacrylamide as the monomers and cross-linker, respectively, and ammonium persulfate as the redox initiator (Sigma-Aldrich, New Zealand).

Dialysis membranes, with a molecular weight cutoff of <15 kDa, were used as the diffusive layer for the liquid-binding layer DGT. The membranes were prepared as in previous studies.<sup>12</sup> The membranes were soaked in deionized water (18.2 MΩ) overnight, washed with 80 °C solution of 0.3 w/v % sodium sulfide for 1 min, soaked in 60 °C deionized water for 2 min, then 0.2 v/v % sulfuric acid, and lastly 60 °C deionized water before being stored in deionized water.<sup>12</sup> The dialysis membrane was then cut into disks (25 mm diameter).

A custom-made liquid-binding phase DGT base was designed using Solidworks (Dassault Systèmes, France) and 3D-printed using an Anycubic Photon printer (Shenzhen, China) and white photocurable resin ( $\lambda = 405$  nm). The

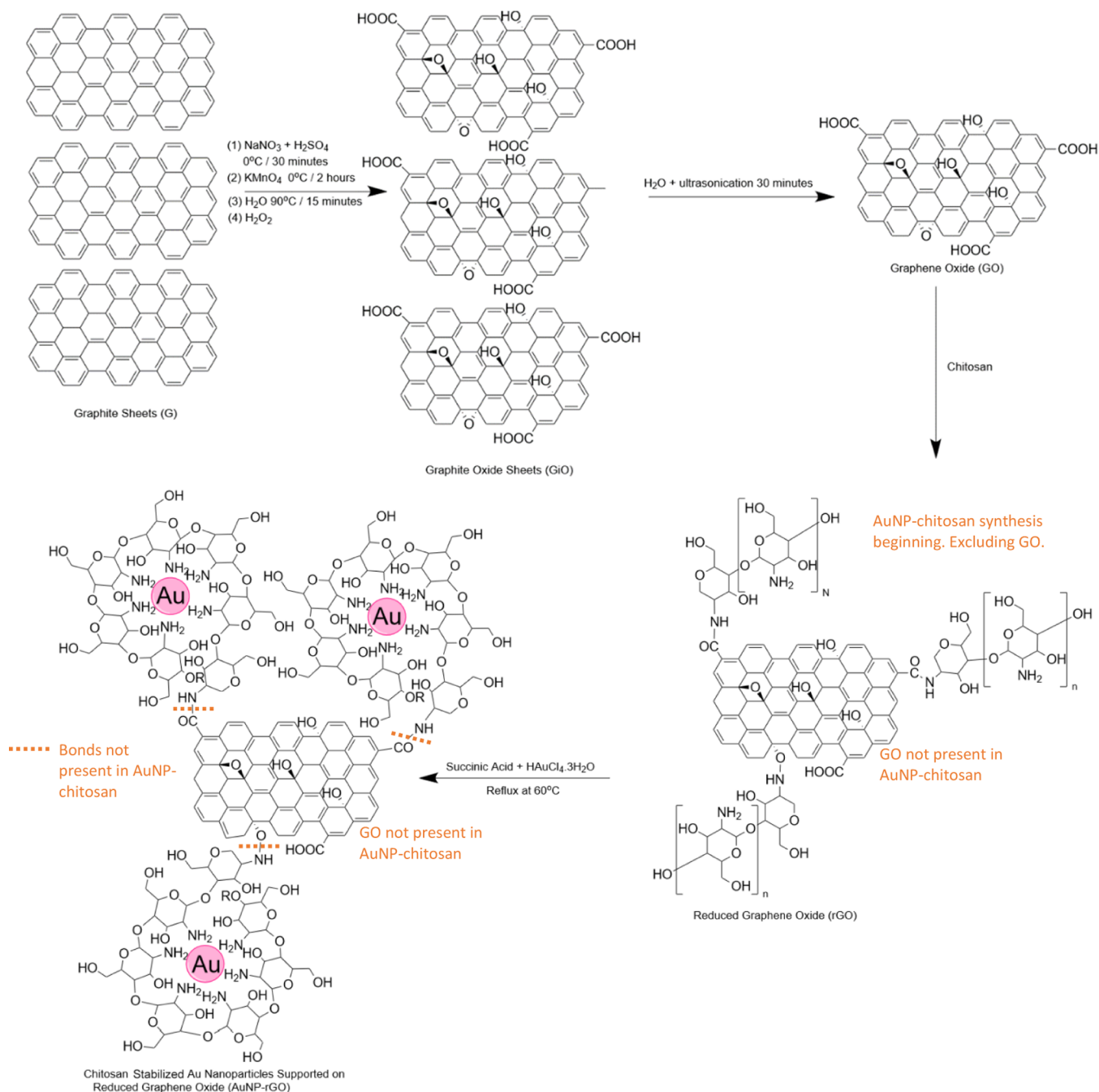


**Figure 2.** Reaction illustration for synthesis AuNP-chitosan and AuNP-rGO and the possible binding modes of the chitosan to the gold.

design was based on the standard DGT solution probe base so that the standard DGT caps fitted and provided a strong seal.

AuNP-chitosan DGTs were assembled by layering the diffusion layer and polyethersulfone filter membrane (0.15 mm) (Sterlitech, Washington, United States) over the binding layer on a custom-made DGT base, before sealing in place with the standard DGT cap (Figure 1A). The Fe(0) reducing hydrogel was layered between the dialysis membrane and filter membrane, in the combined Fe(0)/AuNP-chitosan DGT (Figure 1B). The volume of the liquid-binding layer DGT designed and made here was 2 mL, and 1.5 mL of  $5 \text{ g L}^{-1}$  AuNP-chitosan suspension was used in each liquid-binding layer DGT. The volume of the liquid-binding layer DGT was greater than the AuNP-chitosan suspension to ensure no AuNP-chitosan suspension was lost while the dialysis

membrane and subsequent layers were assembled on the DGT base. Section 2.4 details the preparation of the gold nanoparticle suspension.

**2.2. Zero-Valent Iron Hydrogel Preparation.** P(AMPS/AMA) copolymer hydrogels were prepared via radical polymerization, based on the method developed by Sahiner et al.<sup>21</sup> Briefly, 7.89 mmol (1.6351 g) 2-acrylamido-2-methyl-1-propanesulfonic acid (AMPS) and 0.263 mmol (1 mol % with respect to the total monomer, i.e., AMPS and acrylamide mol sum) *N,N'*-methylenebisacrylamide (0.0203 g) were thoroughly mixed in 3.27 mL (18.41 mmol) of acrylamide and 6.73 mL of deionized water until completely dissolved. 1 mL of 1 w/v % ammonium persulfate was added and thoroughly mixed. The gel solution was carefully pipetted between glass plates separated by 0.5 mm inert spacers to avoid bubbles and

polymerized at 40 °C for ~100 min or until completely polymerized. Gels were carefully removed from the plates and immersed in 750 mL of 0.12 mol L<sup>-1</sup> FeCl<sub>3</sub> solution for 48 h on a shaker plate. The hydrated Fe(III)-impregnated gels were washed in deionized water for 24 h to remove unreacted reagents and physisorbed Fe(III). The water was changed at least three times over that period. The iron(III) solution was prepared with laboratory-grade reagent anhydrous FeCl<sub>3</sub>.

Fe(III) was reduced to Fe(0) with NaBH<sub>4</sub> (~30 mL of 0.16 mol L<sup>-1</sup>) under a nitrogen atmosphere for 2 hours. The sheets were rinsed with N<sub>2</sub>-sparged 18.2 MΩ water, after which they were cut into disks (diameter = 25 mm) for nitrate reduction studies and incorporation into the DGT devices.

**2.3. Nitrate Reduction.** Determination of the total mass of nitrate reduced to nitrite, and other species (NH<sub>4</sub><sup>+</sup>/NH<sub>3(aq)</sub> and NO<sub>x(g)</sub>), is necessary to ensure that enough nitrite is produced to yield color change in the binding layer. Batch reactor nitrate reduction experiments were performed in triplicate, under atmospheric conditions. Briefly, Fe(0)-p(AMPS/AMA) disks were placed in 100 mL of 20 mg L<sup>-1</sup> NO<sub>3</sub><sup>-</sup> (from NaNO<sub>3</sub>). Samples (1 mL) were taken at regular intervals which were diluted with 4 mL of deionized water, to meet the required volume for analysis via ion chromatography. Samples were taken at regular intervals and analyzed for nitrate and nitrite via ion chromatography and ammonia/ammonium via spectrophotometry.<sup>22</sup> Gaseous species were not determined, a nitrogen balance was performed, and the nitrogen unaccounted for by ion chromatography and spectrophotometry was presumed to be NO<sub>x(g)</sub>.

**2.4. Gold Nanoparticle Preparation.** Chitosan-stabilized gold nanoparticles were prepared similarly as previously reported.<sup>17</sup> Briefly, 0.5 g of low-molecular-weight chitosan (150 kDa) was added to 30 mL of deionized water and stirred, and HCl (0.6 mol L<sup>-1</sup>) was added dropwise until the chitosan was dissolved, to which 0.1 mol L<sup>-1</sup> succinic acid and 50 mL of 1 mmol L<sup>-1</sup> HAuCl<sub>4</sub> were added simultaneously, and then heated at 60 °C while stirring under reflux until the color turned wine red.<sup>17</sup> NaOH (0.1 mol L<sup>-1</sup>) was added 1 mL at a time to aid in the formation of the AuNP-chitosan. The AuNP-chitosan nanoparticle composite was oven-dried at 60 °C.

AuNP suspensions were prepared by adding the dried AuNPs to deionized water and alternately sonicated for 15 min and vigorously manually shaken until there were no large AuNP particles in the suspension (determined visually). A chitosan-stabilized AuNP on a reduced graphene oxide (AuNP-rGO) was synthesized alongside the AuNP-chitosan composite.<sup>17,23–25</sup> The AuNP-rGO composite was analyzed alongside the AuNP-chitosan suspension; however, due to poor color development characteristics, it was not pursued beyond basic color testing (full details are in the [Supporting Information](#)). A reaction schematic for the AuNP-chitosan and AuNP-rGO is provided below ([Figure 2](#)).<sup>17,25–27</sup>

**2.5. Diffusion Coefficient.** The presence of Fe in the p(AMPS/AMA) hydrogel network and the use of different monomers to create the hydrogel to the standard APA DGT diffusion layer mean that the diffusion coefficients of nitrate through the Fe(0) hydrogels were different. The diffusion coefficient of nitrate/nitrite through the Fe p(AMPS/AMA) hydrogels and dialysis membrane was determined via horizontal diffusion cell (area = 3.46 cm<sup>2</sup>). The diffusion cell was custom-made from Schott bottles, glass flanges were attached to each bottle, and clamps were used to join the flanges and hold the membranes/hydrogels in place. Chamber

1 contained 130 mL of 80 mg L<sup>-1</sup> NO<sub>2</sub><sup>-</sup> or NO<sub>3</sub><sup>-</sup> (from NaNO<sub>2</sub> and NaNO<sub>3</sub>), and chamber 2 contained 130 mL of deionized water, which were stirred rapidly throughout using magnetic stir bars. NaCl (0.01 mol L<sup>-1</sup>) was used as an ionic adjuster. 1 mL samples were taken each hour for 10 h and were gravimetrically diluted to 4 mL for analysis via ion chromatography. The diffusion coefficient was calculated using the following equation

$$J = \frac{M}{A_p t} = \frac{D_g C}{\delta_g} \quad (1)$$

$$\frac{D_1 \eta_1}{T_1^K} = \frac{D_2 \eta_2}{T_2^K} \quad (2)$$

where  $J$  = flux (mg cm<sup>-2</sup> s<sup>-1</sup>),  $M$  = mass (mg),  $A_p$  = diffusion window area (cm<sup>2</sup>),  $t$  = time (s),  $D_g$  = diffusion coefficient through gel (cm<sup>2</sup> s<sup>-1</sup>),  $c$  = concentration (mg cm<sup>-3</sup>), and  $\delta_g$  = thickness of the hydrogel (cm).<sup>10</sup> The Stokes–Einstein equation ([eq 2](#)) links the temperature dependence of the diffusion coefficients to the viscosity of water,<sup>10</sup> where  $\eta$  = the viscosity of water (mPa s<sup>-1</sup>),  $D$  = the diffusion coefficient (cm<sup>2</sup> s<sup>-1</sup>), and  $T^K$  = the absolute temperature (K).<sup>10</sup> Diffusion coefficients were temperature-corrected ([eq 3](#)), and diffusive boundary layer (DBL) calculations were performed as described by Davison.<sup>10</sup>  $T$  = temperature (°C),  $D_T$  = diffusion coefficient at temperature  $T$  (cm<sup>2</sup> s<sup>-1</sup>), and  $D_{25}$  = diffusion coefficient (cm<sup>2</sup> s<sup>-1</sup>) at 25 °C.<sup>10</sup>

$$\log D_T = \frac{1.37023(T-25) + 0.000836(T-25)^2}{109 + T} + \log \frac{D_{25}(273 + T)}{298} \quad (3)$$

The diffusion coefficient of nitrate through the APA diffusion layer was 1.46 × 10<sup>-5</sup> cm<sup>2</sup> s<sup>-1</sup> at 25 °C.<sup>28</sup> The diffusion coefficient of nitrate and nitrite through water was 1.70 × 10<sup>-5</sup> cm<sup>2</sup> s<sup>-1</sup> at 25 °C.<sup>29</sup>

The thickness of the dialysis membrane after pretreatment and the Fe p(AMPS/AMA) hydrogels was measured using a WILD M38 microscope (Heerbrugg, Switzerland) with a Nikon Digital Sight DS-U1 camera (Tokyo, Japan) and analyzed using Image-Pro Plus (Media Cybernetics, Maryland, United States).

**2.6. Color Determination, Stability, and Competing Ions.** To determine the optimal AuNP-chitosan concentration for color development, a series of experiments were conducted. First, nitrite solution, prepared from NaNO<sub>2</sub>, was added to vials of freshly prepared AuNP-chitosan suspension, to provide NO<sub>2</sub><sup>-</sup> masses from 0 to 145 μg and AuNP concentrations of 1, 3, and 5 g L<sup>-1</sup>, providing a total volume of 1.5 mL. The vials were placed in a plastic holder and on a shaker plate. The maximum nitrite mass was chosen because it was similar to the previously reported binding capacities of the standard nitrate DGT.<sup>30,31</sup> Second, the AuNP suspensions were reanalyzed 7, 14, and 21 days after the initial analysis to determine the stability of the AuNP suspensions when reacted with nitrite.

The color response of the AuNP-chitosan suspension was tested by the addition range of competing ions (NO<sub>3</sub><sup>-</sup>, HPO<sub>4</sub><sup>2-</sup>, SO<sub>4</sub><sup>2-</sup>, HCO<sub>3</sub><sup>-</sup>, and Cl<sup>-</sup>, from NaNO<sub>3</sub>, K<sub>2</sub>HPO<sub>4</sub>, Na<sub>2</sub>SO<sub>4</sub>, NaHCO<sub>3</sub>, and NaCl). Competing ion solution was pipetted into 1.5 mL glass reaction vessels along with AuNP-

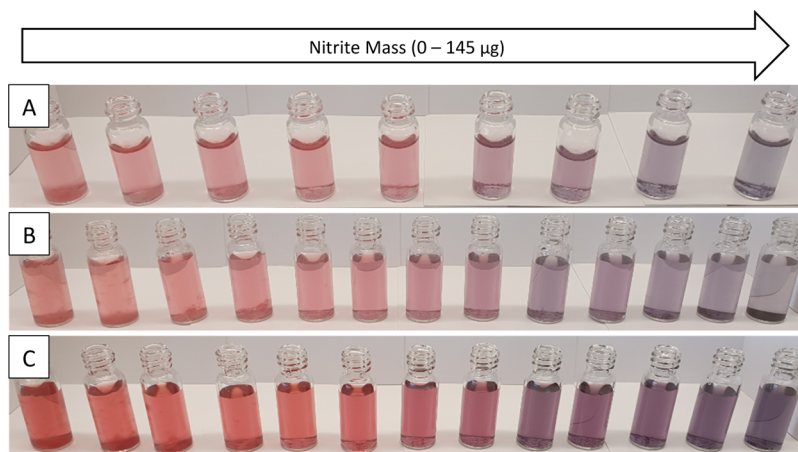


**Figure 3.** Image of (A) 1, (B) 3, and (C) 5 g L<sup>-1</sup> AuNP-chitosan reacted with a range of nitrite masses (0–145 µg).

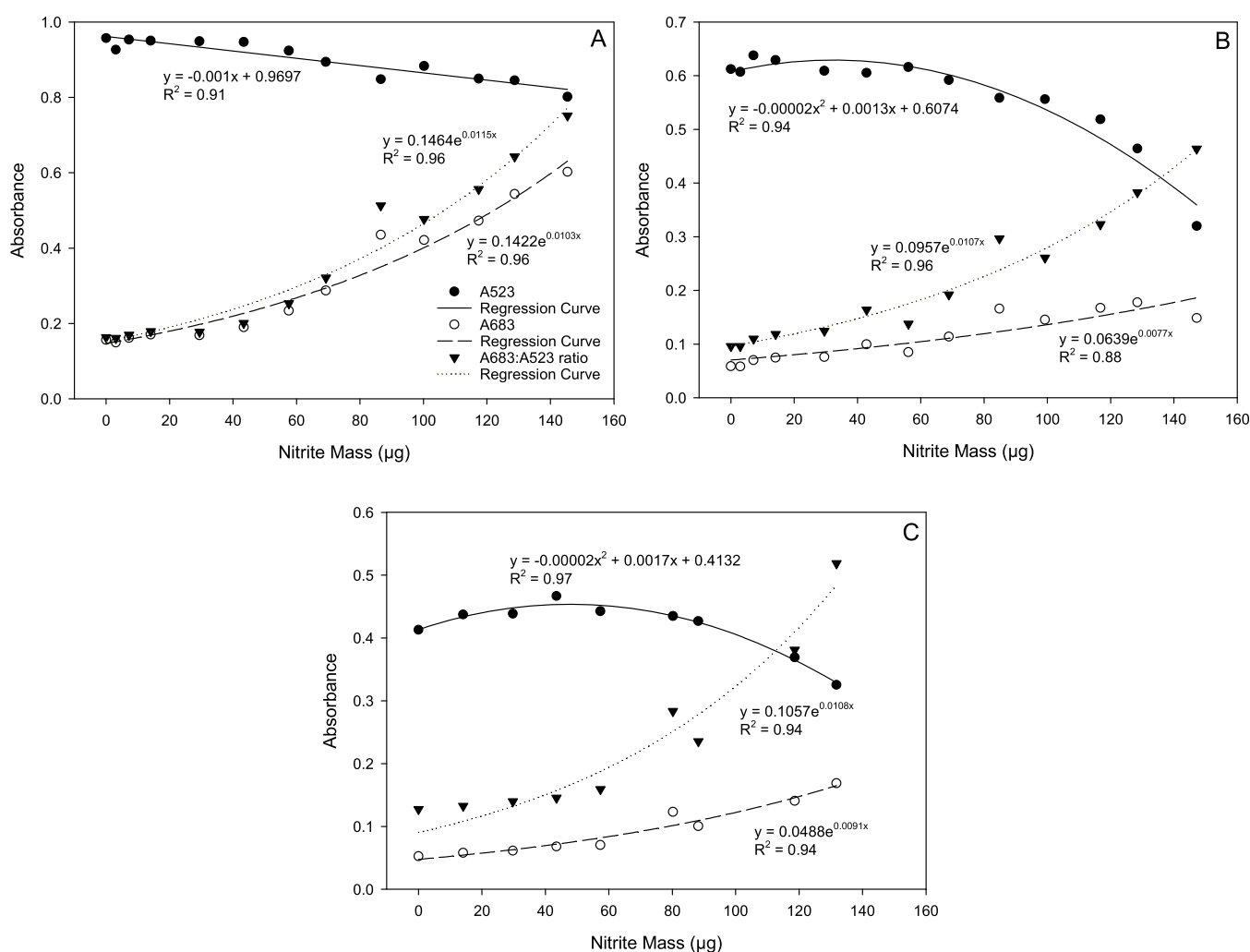


**Figure 4.** UV-vis absorbance for (A) 5, (B) 3, and (C) 1 g L<sup>-1</sup> AuNP-chitosan reacted with a range of nitrite masses (0–145 µg).

chitosan (5 mg L<sup>-1</sup>) such that their concentrations were 1, 5, 10, 20, and 50 mg L<sup>-1</sup>.

Liquid-binding layer AuNP-chitosan DGTs, Figure 1A, were deployed in a range of nitrite solutions (volume = 6 L) to determine whether a color change could be induced within the DGT probe. Furthermore, the extent to which the AuNP-chitosan liquid-binding layer met the theoretical requirements

for DGT, of rapid and strong adsorption to maintain the concentration gradient through the material diffusion layer (MDL),<sup>10</sup> was assessed. AuNP-chitosan DGTs were deployed in triplicate for 5 days in nitrite solutions from 0 to 1000 mg L<sup>-1</sup> NO<sub>2</sub><sup>-</sup> (prepared from NaNO<sub>2</sub>). To establish the efficacy of the combined Fe(0)-p(AMPS/AMA) hydrogel and AuNP-chitosan DGT (Figure 1B), the combined DGTs were

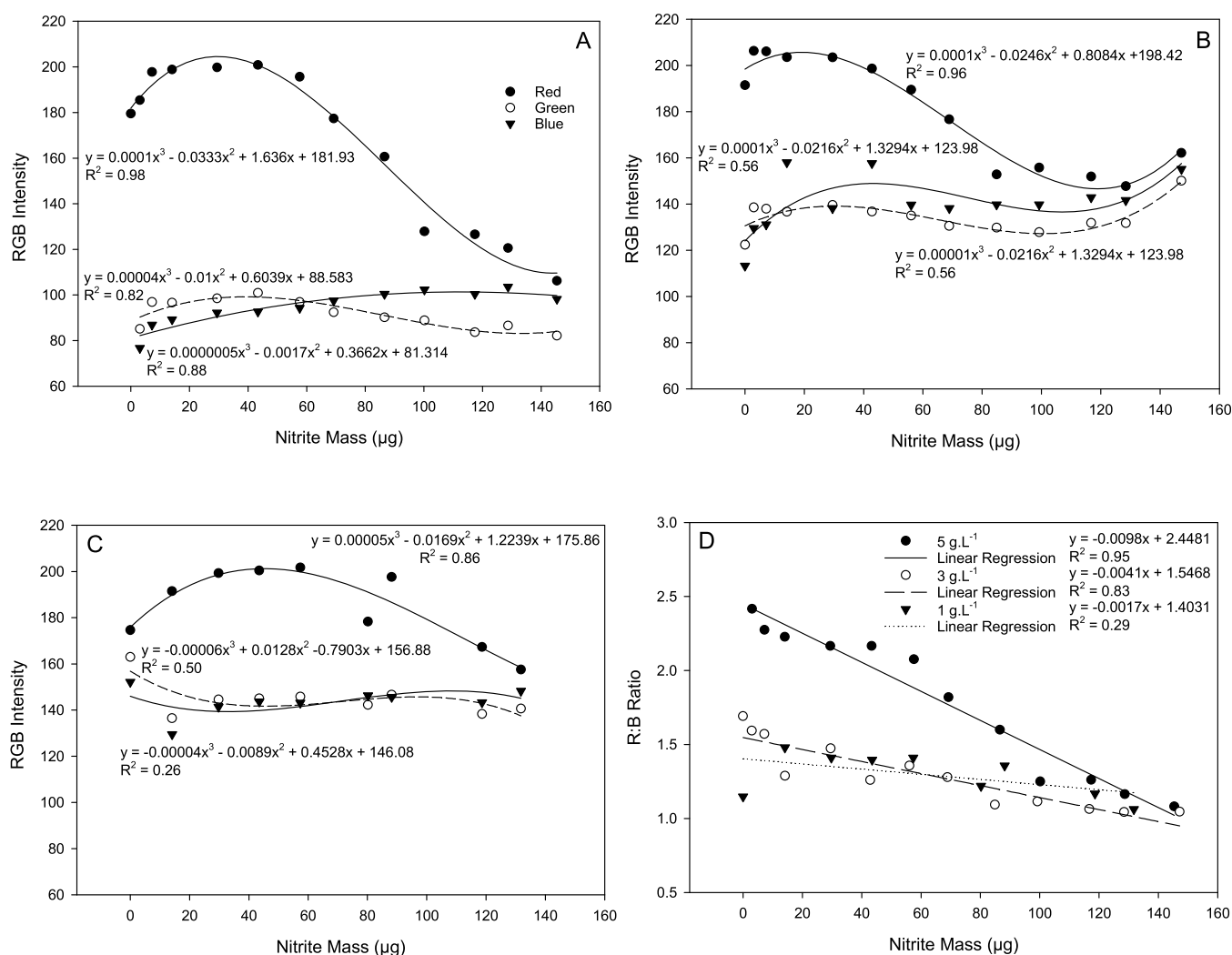


**Figure 5.** Red, green, and blue (RGB) intensities vs the nitrite mass for (A) 5, (B) 3, and (C) 1 g L<sup>-1</sup> AuNP-chitosan. (D) Ratio of red to blue intensity for varying concentrations of AuNP-chitosan (1, 3, and 5 g L<sup>-1</sup>) reacted with different masses of nitrite, and the linear regression of the red/blue ratio to nitrite mass.

deployed in nitrate solutions (volume = 6 L) of various concentrations (10, 20, and 50 mg L<sup>-1</sup>). In both experiments, the solutions were stirred using magnetic stir bars, temperature was logged throughout using an Xplorer GLX (PASCO Scientific, California, United States), and solution samples (4 mL) were taken periodically for analysis via ion chromatography.

UV-vis spectroscopy was performed on the AuNP-chitosan, using undiluted AuNP samples in a 1 mL quartz cuvette, to determine the color intensity, and blue shift when reacted with nitrite. The AuNP suspensions were photographed using a Samsung S10 mobile phone camera. The RGB (red, green, and blue) composition was analyzed using ImageJ. Vials were placed on a white cardboard photobooth, in a fume hood, and the fume hood lighting was used to illuminate the samples. This setup was chosen because of its simplicity and ease of replication.

**2.7. Analysis.** Scanning electron microscopy (SEM) images, using a Hitachi S-4700 field emission SEM, were taken of the Fe-impregnated p(AMA/AMPS) hydrogels and the AuNP-chitosan. The Fe hydrogels were imaged prereduction to Fe(0) and post nitrate reduction. Fourier transform infrared (PerkinElmer Spectrum 100) and powder X-ray

diffraction (Panalytical Empyrean) spectroscopy of the AuNP-chitosan (and other synthesized Au compounds and graphene oxide supports) were also performed.<sup>17,32,33</sup>

Analysis of solution nitrate and nitrite concentrations was performed using ion chromatography.<sup>30</sup> Ammonium/ammonia concentrations were determined using a spectrophotometer (Jenway 7300, United Kingdom).<sup>22</sup> Two reagent solutions were prepared for colorimetric determination of ammonium/ammonia. Reagent solution 1 was 1 L of 10 g L<sup>-1</sup> phenol and 50 mg L<sup>-1</sup> sodium nitroprusside.<sup>22</sup> Solution 2 contained 5 g of NaOH and 8.4 mL of 5% NaOCl, which was made to 1 L with deionized water. Both solutions were stored in brown Schott bottles, refrigerated, and aged for 2 days before use. 2 mL of both reagents was added to 2 mL of the sample, which was subsequently heated in a temperature bath (37 °C) for 15 min, before being transferred to 5 mL plastic cuvettes for spectrophotometric analysis alongside calibration samples.

### 3. RESULTS

**3.1. AuNP-Chitosan Development and Color Response.** An AuNP-chitosan suspension was developed, which provided a quantitative color response to varying nitrite masses (0–145  $\mu\text{g}$  of nitrite in 1.5 mL of the AuNP-chitosan

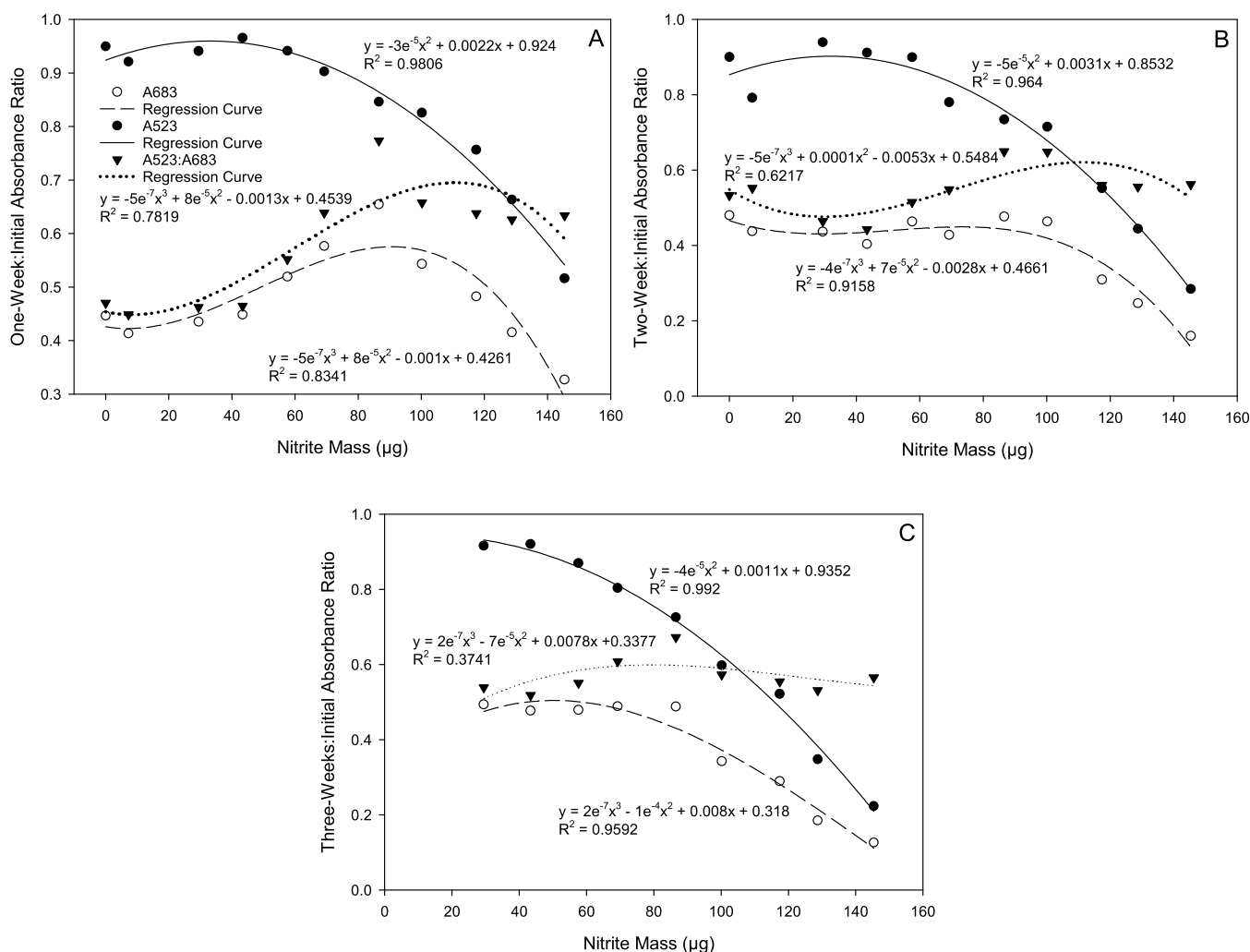


**Figure 6.** Stability of  $5 \text{ g L}^{-1}$  AuNP-chitosan suspensions determined by UV-vis at 523 and 683 nm and the 683:523 nm ratio compared to the initial  $5 \text{ g L}^{-1}$  AuNP-chitosan suspensions (Figure 4C). Stability was determined as the ratio of these components for (A) 1 week after initial analysis, (B) 2 weeks after the initial analysis, and (C) 3 weeks after the initial analysis.

suspension) (Figures 3–5). The color response was dependent on the AuNP-chitosan concentration.

Increasing the AuNP-chitosan concentration made visual determination of the color change easier (Figure 3). The color change was more distinct, providing stronger UV-vis absorbance at 523 and 683 nm, as the suspension became blue-shifted in the presence of nitrite (Figure 4). The higher concentration of AuNP-chitosan also provided stronger UV-vis calibration curves (greater absorbance), with improved  $R^2$  values (Figure 4A–C). There was no significant color change within the AuNP-rGO suspensions and yielded poorly correlated UV-vis and RGB regression curves (Supporting Information Figure S1). AuNP hydrogels were also developed, but they did not change color in the presence of nitrite, determined visually and via UV-vis, as such, they were not pursued.

As the mass of nitrite approached the maximum detection limit, the AuNPs precipitated out of solution, accumulating in the bottom of the vials (Figure 3). The intensity of the color of the AuNP suspension decreased, until all AuNPs precipitated, and the solution became colorless—the UV-vis peaks disappeared. Increasing the concentration of the AuNP suspension increased the mass of nitrite required for all

AuNPs to precipitate out of solution and therefore the upper detection limit.

The reaction of the AuNP-chitosan with large ( $>100 \mu\text{g}$ ) nitrite masses formed a precipitate which settled to the bottom of the vials; however, unlike the AuNP-rGO, layers of varying color intensity within the suspension were not formed (Figure 3A–C, and Supporting Information Figure S1). It was, therefore, easier to take consistent samples for UV-vis and RGB analysis, producing regression curves with higher  $R^2$  values (Figures 4 and 5).

The best-fit regression curves for the RGB analyses were cubic polynomials (Figure 5). RGB analysis therefore required the combination of at least two components because single components could provide multiple different nitrite masses. The components chosen were red and blue because they provided the greatest difference in intensity compared to the blank AuNP suspension, except for  $1 \text{ g L}^{-1}$  AuNP-chitosan. The ratio of the red-to-blue components provided the strongest correlation to mass as the AuNP-chitosan concentration increased (Figure 5D).

Due to the improved color reaction of the  $5 \text{ g L}^{-1}$  AuNP-chitosan suspension, compared to lower concentrations and the AuNP-rGO suspension (Supporting Information Figure

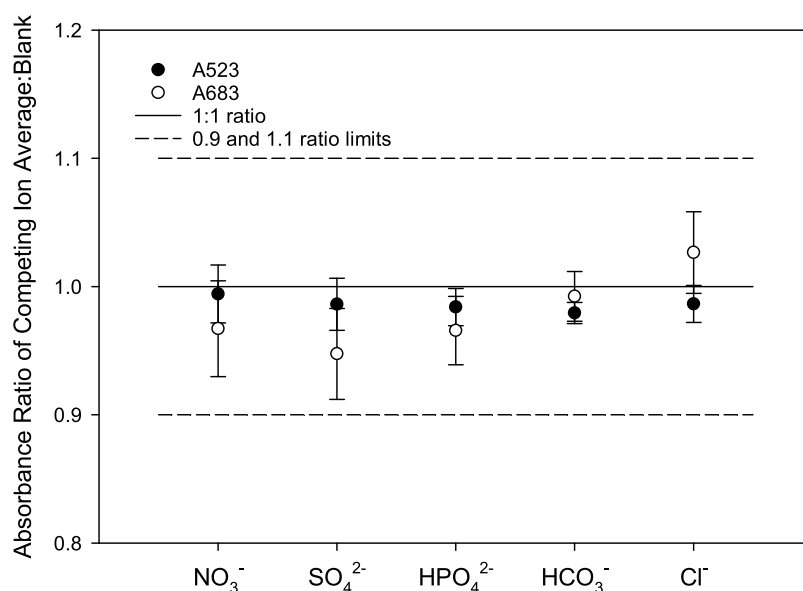


**Figure 7.** Color response of the AuNP-chitosan suspension in the presence of potentially competing ions. Ratio given as average UV–visible adsorption of the AuNP-chitosan suspension (523 and 683 nm) for each competing ion to the AuNP-chitosan suspension alone (blank). Bars show the standard deviation from average (mean).

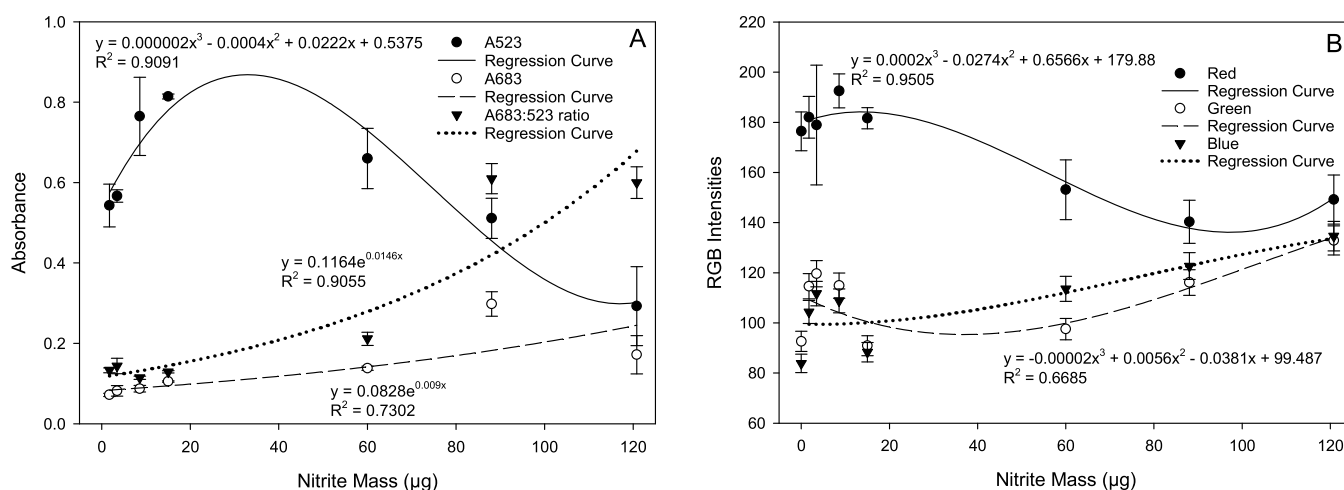


**Figure 8.** (A) UV–vis and (B) RGB analyses of AuNP-chitosan DGT for laboratory deployments in synthetic solutions of various nitrite concentrations. Nitrite mass is the mass of nitrite within the binding layer. The same curve types were fitted as for the AuNP suspension data (Figures 4 and 5).

S1), subsequent color development experiments (stability and solution) utilized the 5 g L<sup>-1</sup> AuNP-chitosan suspension alone.

### 3.2. AuNP-Chitosan Stability and Competing Ions.

The color development continued after the initial analysis (Figure 6). The absorbance ratio of 1 week, 2 weeks, and 3 weeks after initial analysis to the initial analysis is <1 for all components (red 523 nm, blue 683 nm, and 683:523). The 523 nm ratio decreased as the nitrite mass increased because the higher nitrite mass vials continued developing to a greater extent (blue shifting). One week after the initial analysis, the lower nitrite mass vials began forming “globules”, the same color as the suspension. The globules formed due to the agglomeration of chitosan and not the nanoparticles. The “globules” were not significantly blue-shifted, which would result from the precipitation of the AuNP-chitosan. The increased mass of nitrite appears to stabilize the AuNP suspension by reducing the aggregation of the chitosan. The AuNP-rGO suspension and lower AuNP-chitosan provided

weaker curve fits and were significantly blue-shifted due to continued color development (example figure provided in the Supporting Information).

The AuNP-chitosan suspension was highly selective for nitrite. The potentially competing ions tested (NO<sub>3</sub><sup>-</sup>, SO<sub>4</sub><sup>2-</sup>, HPO<sub>4</sub><sup>2-</sup>, HCO<sub>3</sub><sup>-</sup>, and Cl<sup>-</sup>) provided UV–visible adsorption values which closely correlated to the blank AuNP-chitosan adsorption values at both 523 and 683 nm (Figure 7). If a color response occurred, the adsorption at 523 nm would significantly decrease and the adsorption at 683 nm would increase.

**3.3. AuNP-Chitosan DGT Development and Solution Trials.** 5 g L<sup>-1</sup> AuNP-chitosan suspensions, as presented above, were determined to be the optimal concentration for use within the liquid-binding layer DGT. Subsequent solution trials of the assembled AuNP-chitosan DGT, therefore, utilized 1.5 mL of 5 g L<sup>-1</sup> AuNP-chitosan suspension per DGT as the liquid-binding layer. Color change within the liquid-binding



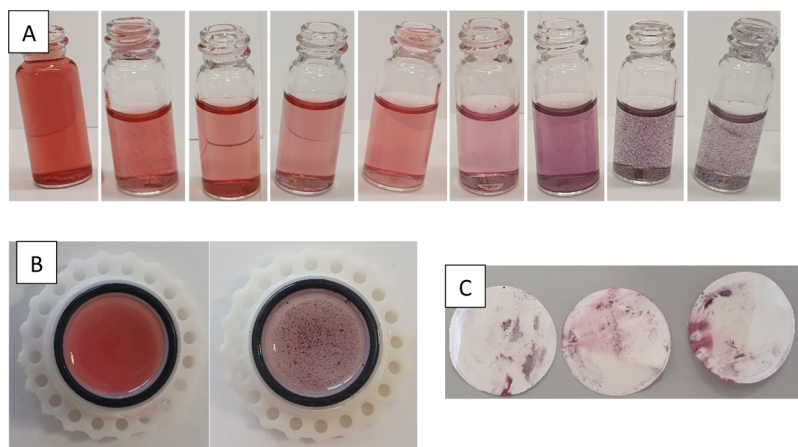


**Figure 9.** (A) AuNP suspension in 3D-printed liquid-binding layer DGT. (B) AuNP suspensions after deployment in liquid-binding layer DGT in nitrite solutions (0 and 90  $\mu\text{g}$ ). (C) Formation of AuNP precipitates on the dialysis membranes where the nitrite mass in the binding layer was large (>90  $\mu\text{g}$ ).

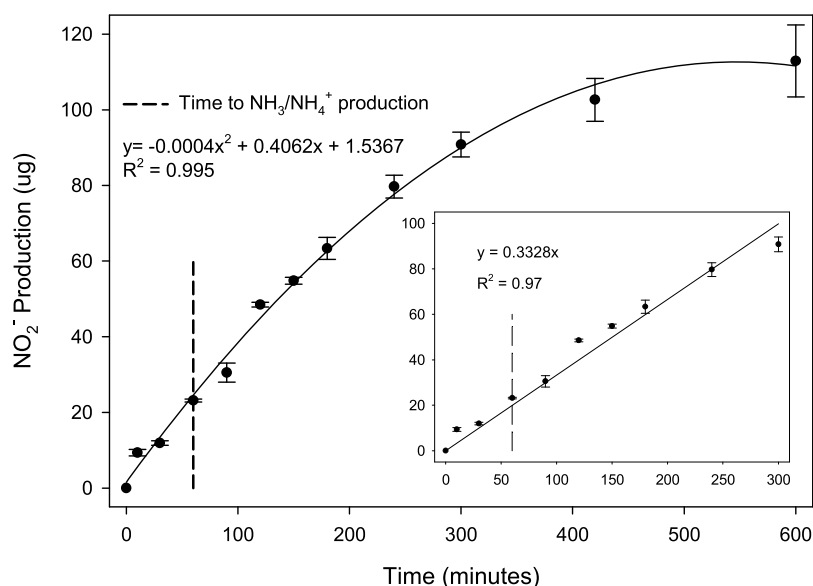


**Figure 10.** Nitrate reduction (nitrite production) with Fe(0)-p(AMPS/AMA) hydrogel (10% AMPS) and inset of linear reduction.

layer was achieved in situ during solution trials (Figures 8 and 9). Unfortunately, the color development was not rapid enough to meet the main theoretical requirement of DGT, rapid adsorption/reaction to the binding layer to maintain the concentration gradient.<sup>34</sup> Development of full color occurred over several days, for combination of the AuNP-chitosan DGT with the Fe(0) reducing layer. This was confirmed via deployment of the combined Fe(0)-p(AMPS/AMA) and AuNP-chitosan DGT in nitrate solutions of various concentrations, where the AuNP did not measurably change color (figure not supplied).

The AuNP-chitosan suspension color change was clearly detectable visually after deployment of the AuNP-chitosan DGT in various nitrite solutions (Figures 8 and 9). The color change was also clearly detectable in the DGT probes, after the MDL was removed (Figure 9B). The blue shift due to the decrease in the AuNP distance in the presence of nitrite was easily detectable visually (Figure 8). The formation of AuNP-chitosan aggregates occurred at high nitrite (90–120  $\mu\text{g}$ ) masses (Figure 9A,B). AuNP-chitosan aggregates also formed

on the dialysis membrane after deployments in high concentration nitrite solutions (Figure 9C).

Dilution of the AuNP-chitosan suspension occurred during solution deployments, and the UV-vis (523 and 683 nm) ratio of the AuNP-chitosan suspension in AuNP-DGT deployed in 0  $\text{mg L}^{-1}$  nitrite to the undeployed AuNP-chitosan suspension was 0.69 and 1.01, respectively.

**3.4. Nitrate Reduction and Diffusion Layer Properties.** Figure 10 illustrates the production of nitrite by the Fe(0)-p(AMPS/AMA) hydrogel. Reduction began immediately upon introduction of the Fe(0) hydrogel to the reaction vessel. Ammonia and ammonium production was determined experimentally (data not provided) and lagged behind nitrite production by 60 min—in the absence of an adsorbent to remove the produced nitrite. A full nitrogen mass balance indicated that  $\text{NO}_{x(g)}$  species were likely produced, beginning at approximately the same time as the ammonia and ammonium production and accounted for nearly 90% of the total difference between the initial nitrate-N and the nitrate-N at 600 min.  $\text{NO}_x$  species, however, were not determined experimentally.

The diffusion coefficients of nitrite and nitrate through the Fe(III)-p(AMPS/AMA) hydrogel were both  $1.24 \times 10^{-5} \text{ cm}^2 \text{ s}^{-1}$  at 20.6 °C, and at temperature corrected to 25 °C, they were  $1.40 \times 10^{-5} \text{ cm}^2 \text{ s}^{-1}$ . This is 95.8% of the diffusion coefficient of nitrite through water at 25 °C ( $14.6 \times 10^{-6} \text{ cm}^2 \text{ s}^{-1}$ ).<sup>29</sup> The thickness of the Fe(III)-p(AMPS/AMA) hydrogel after washing and swelling was 1.1 mm. The diffusion coefficients of nitrite and nitrate through the dialysis membrane were  $4.65 \times 10^{-6} \text{ cm}^2 \text{ s}^{-1}$  at 21.9 °C and  $4.56 \times 10^{-6} \text{ cm}^2 \text{ s}^{-1}$  at 20.4 °C, and at temperature corrected to 25 °C, they were  $5.05 \times 10^{-6} \text{ cm}^2 \text{ s}^{-1}$  and  $5.15 \times 10^{-6} \text{ cm}^2 \text{ s}^{-1}$ , respectively. This is 34.6 and 35.4% of the diffusion coefficient of nitrite through water at 25 °C. The thickness of the dialysis membrane after pretreatment was 43  $\mu\text{m}$ .

## 4. DISCUSSION

A AuNP-chitosan colorimetric technique was developed and incorporated into a custom-designed and 3D-printed DGT probe, as a liquid-binding layer. This approach provided quantitative nitrite masses between 0–145  $\mu\text{g}$  during batch and bulk solution testing. A poly-2-acrylamido-2-methyl-1-propanesulfonic acid/acrylamide (p(AMPS/AMA)) copolymer hydrogel was developed and impregnated with Fe(III) which was reduced to Fe(0) nanoparticles. The Fe(0)-p(AMPS/AMA) hydrogel was used to reduce nitrate to nitrite, for determination with the AuNP-chitosan suspension. Despite the success of these individual steps, there are a number of challenges remaining (discussed below), such as resolving the insufficiently fast reaction rate of the AuNP-chitosan suspension so that DGT theoretical requirements are met. The combination of the combined AuNP-chitosan and Fe(0) systems was unsuccessful, likely due to the slow AuNP-chitosan reaction rate. If constraints imposed by slow reaction rates are resolved, this system could offer a new DGT which quantitatively changes color in situ in response to nitrate in solution.

**4.1. AuNP-Chitosan DGT.** Color change within the binding layer of the AuNP-chitosan DGT was achieved in situ in laboratory-based experiments, during deployment in nitrite solutions of various concentrations (0–1000  $\text{mg L}^{-1}$ ). The determined masses were significantly lower, however, than the expected masses. This was likely due to the dilution of the AuNP-chitosan suspension, and the rate of reaction of the AuNP-chitosan suspension was not rapid enough to meet the theoretical requirements of DGT (discussed below). The color change was most easily discernible, via both UV–vis and RGB analysis, at nitrite masses greater than 40  $\mu\text{g}$ ; however, nitrite masses from 0 to 120  $\mu\text{g}$  were successfully determined. The combination of the Fe(0)-p(AMPS/AMA) and AuNP-chitosan systems was unsuccessful, with no measurable color change occurring upon deployment in nitrate solutions of various concentrations. This was likely due to the slow reaction rate of the AuNP-chitosan suspension. The nitrite produced by the Fe(0)-p(AMPS/AMA) hydrogel formed an equilibrium with the bulk solution as it was not rapidly removed by the AuNP-chitosan-binding layer. The nitrite mass produced was diluted by the bulk solution such that the nitrite concentration was too low for a measurable color change in the AuNP-chitosan suspension. In some of the combined DGT, furthermore, the Fe(0) hydrogel expanded upon oxidation to Fe(III) so that the hydrogel broke the seal between the O-ring and the dialysis membrane and the AuNP-chitosan suspension diffused into the bulk solution. The expansion of the Fe-

hydrogel upon oxidation and subsequent loss of seal between the O-ring and dialysis membrane could potentially be overcome by the development of a single pot reduction/color reaction in future studies (discussed below).

Preconcentration of the AuNP-chitosan suspension with small mass of nitrite (<40  $\mu\text{g}$ ), prior to construction of the DGT, could make determination of low nitrite concentrations easier. The color change was the greatest above  $\sim 40 \mu\text{g}$  of nitrite, and it was difficult to visually discern differences in nitrite masses below  $\sim 40 \mu\text{g}$  (Figures 4–8). The presence of nitrite also appeared to stabilize the AuNP-chitosan suspension (discussed in Section 4.2). Extremely high nitrite masses, however, appeared to be a potential issue for the deployment of AuNP-chitosan DGT due to the precipitation of the AuNP-chitosan on the dialysis membrane (Figure 9C).

Aggregation of the AuNPs due to the presence of large masses of nitrite led to the precipitation of blue-shifted AuNPs on the dialysis membrane. As further discussed in Section 4.3, this precipitation will affect the MDL thickness and present practical challenges for the field deployment of AuNP-chitosan DGT—although these effects were not examined in this study.

A DGT base for housing the AuNP suspension, and other liquid-binding layers, was designed and 3D-printed with total volume (excluding the volume created by extrusion of the rubber O-ring) of 2 mL (Figure 9B). The AuNP-chitosan volume used in the DGT was 1.5 mL; the added volume meant that layering the dialysis membrane and other layers of the MDL was a simple process. Smaller volume probes were also constructed, but it was difficult to stop the AuNP suspension from being drawn out while the MDL was assembled. This meant that the AuNP-chitosan DGT needed to be deployed with the aperture window facing down so that the AuNP-chitosan suspension was in full contact with the MDL. The base was designed to operate with the push-fit standard DGT solution probe cap. A screw on cap was also designed and tested; however, the torsion force required to seal the dialysis membrane and rubber O-ring led to tearing of the dialysis membrane.

The seal of the push-fit cap provided a strong seal, when combined with the low-molecular-weight cutoff dialysis membrane (<15 kDa). The DGT remained sealed during vigorous shaking. There was, however, dilution of the AuNP-chitosan suspension during deployment, most clearly observed in the decrease in the adsorption at 523 nm of the AuNP-chitosan suspension of DGT deployed in 0  $\text{mg L}^{-1}$  nitrite solution. The volume within the DGT base did not change. The dilution was either due to leakages between the rubber O-ring and dialysis membrane or diffusion of AuNP-chitosan particles through the dialysis membrane. The dilution was likely a consequence of sonicating the AuNP-chitosan during the preparation of the suspension. Sonication has been reported as a method for the fragmentation of chitosan,<sup>35</sup> producing smaller particles that could diffuse through the dialysis membrane. The formation of the AuNP-chitosan suspension in a stronger solvent, instead of deionized water, may remove the need for sonication.

**4.2. Color Reaction.** Color development occurred slowly; all samples were initially analyzed 7 days after the introduction of nitrite. Perceivable color change did not occur until about 4 days. The color change is induced by the shortening of the AuNP interparticle distance,<sup>18</sup> in the presence of nitrite. Whether the AuNP-chitosan suspension meets the theoretical requirements for application in DGT, rapid, and strong

binding<sup>10</sup> is determined by the rate at which nitrite is bound to the AuNP-chitosan. Presently, color development of the AuNP-chitosan suspension must occur after nitrite is bound, and nitrite must be bound strongly, to meet the theoretical requirements of DGT. It seems, however, that the binding of nitrite and the color change is simultaneous, meaning that the binding of nitrite is not rapid. If this is correct, then the AuNP-chitosan DGTs likely operate under diffusional equilibrium theory (DET) and functionally similar to pore-water samplers, whereby the nitrite concentration in the binding layer is in equilibrium with the concentration of the bulk solution.<sup>13,36</sup>

The AuNP-chitosan suspension showed strong selectivity for nitrite, over the major potential competing ions ( $\text{NO}_3^-$ ,  $\text{SO}_4^{2-}$ ,  $\text{HPO}_4^{2-}$ ,  $\text{HCO}_3^-$ , and  $\text{Cl}^-$ ) (Figure 7). This is necessary for the in-field application of the AuNP-chitosan DGT, as a range of potentially competing ions will be present in natural solution. In comparison, the standard A520E nitrate-DGT is less selective and has been shown to adsorb both nitrite and sulfate.<sup>30,31</sup> The A520E DGT, however, rapidly adsorbs nitrate, provides quantitative nitrate concentrations in a range of solution pH, conductivities, and competing ion concentrations, and has been successfully deployed in natural solutions and denitrifying bioreactors.<sup>30,31</sup>

Coagulation of the AuNP-chitosan suspension occurred at low nitrite concentrations—likely due to the agglomeration of chitosan and not the nanoparticles. The coagulants were not significantly blue-shifted, which would result from the precipitation of the AuNP-chitosan. Chitosan is soluble in acidic solutions ( $\text{pH} < 6$ ); acids protonate the deacetylated units of chitosan, enabling the formation of thin chitosan coatings in solution.<sup>37</sup> Dissolved chitosan chains, however, may preserve a degree of aggregation due to the presence of residual *N*-acetyl groups in the chitosan chain.<sup>37</sup> The deacetylated groups may also form intra- and intermolecular bonds via hydrogen bonding.<sup>37</sup> This deterioration in the chitosan coating of the AuNPs could lead to agglomeration.<sup>37</sup> The increased mass of nitrite, furthermore, appeared to stabilize the AuNP suspension, potentially by reducing the agglomeration of the chitosan. The formation of coagulants in deployed AuNP-DGT is a good and immediate test as to whether the DGT will provide quantitative data.

**4.3. Advantages and Disadvantages.** Liquid-binding phase DGTs were pursued to retain the necessary mobility for the AuNP systems. Liquid-binding phase DGTs have been reported previously;<sup>12,14</sup> the system developed here builds on this previous work. Utilizing liquid-binding phase DGTs presents their own advantages and disadvantages compared to the standard hydrogel-based DGT-binding layers.

Standard DGTs commonly utilize an analyte-selective resin suspended in a polyacrylamide hydrogel as a binding layer.<sup>10</sup> The suspension of AuNPs in an APA network was also explored here. AuNP hydrogels were successfully produced via the hydrogel formation in the particle suspension method and analyzed via UV-vis with altered plastic cuvettes. The AuNP hydrogels, however, did not produce a color change in the presence of nitrite. This was likely due to the decreased mobility of the AuNPs in the hydrogel framework, even though swelled APA gels are ~90% water. The AuNP systems utilized were based on the aggregation mechanism, and the decreased mobility meant that the interparticle distance could not decrease in the presence of nitrite, necessary to illicit a color change.

A potential advantage of the liquid-binding phase DGTs is that they may better meet the assumption that analyte concentration is zero, or negligibly small, at the diffusion layer<sup>34</sup>—binding layer interface. As adsorption sites are occupied on the binding layer, target species would need to travel further into the binding layer to become bound, potentially extending the concentration gradient into the binding layer. If the AuNP-DGTs are not absolutely fixed during deployment, the movement of DGTs continuously mixes the AuNP suspension, ensuring that there are a greater number of binding sites at the diffusion layer/binding layer interface. Mixing of the AuNP suspension could also be diffusion-driven. There is also no waste of potentially expensive reagents, unlike when cutting disks from sheets as with hydrogel-binding layers—the specific volume of binding reagents/color reagents can be pipetted into DGT base.

As previously reported, A520E-DGTs were stable for several days and the binding layer can be dried before or after deployment and provide the same concentration.<sup>30</sup> This is an advantage of the standard nitrate-DGTs over the AuNP systems. Color development was a continuous gradual process; therefore, the samples need to be analyzed after a specific time period (7 days after the introduction of nitrite) or the samples calibrated against calibrations of the same age. The strongest calibrations, however, were produced after 7 days, as the samples degenerated the color and the suspensions became less stable. As discussed in Section 4.2, coagulation of the chitosan can occur if the samples are left for long periods before analysis or the AuNPs could precipitate.

Coagulation will have practical implications for the deployment of AuNP-DGTs. For example, if the deployment period is long, and/or nitrate concentration high, AuNP-nitrite precipitate could form on the dialysis membrane as it did during the laboratory testing, extending the diffusion layer. DGT studies have reported biofouling on the membrane, where it meets bulk solution, which affected the analyte mass that diffused through to the binding layer and therefore the calculated concentration.<sup>38</sup> This could potentially be overcome through the calculation of an effective DBL, whereby the effect the fouling has on the boundary layer is added to the DBL.

**4.4. Formation of AuNPs.** High-molecular-weight chitosan was used to ensure that the final product was sufficiently large that it would not diffuse through the MDL. Although the dialysis membrane had a molecular weight cutoff of 15 kDa and the chitosan used had a molecular weight of 150 kDa, dilution of the AuNP-chitosan suspension occurred when the AuNP-DGTs were deployed in solution. As discussed above, this was likely due to fragmentation of chitosan during sonication.<sup>35</sup> Dissolution, furthermore, of the high-molecular-weight chitosan required the addition of an acid. HCl was chosen because the chloride would not interfere in the reaction. The addition of HCl to dissolve the chitosan necessitated the addition of  $\text{OH}^-$  (from NaOH). The dissolution of chitosan requires increasingly acidic conditions as the molecular weight increases,<sup>39</sup> and use of lower-molecular-weight chitosan may reduce the need for an acidic solvent and sonication of the AuNP-chitosan product, while still being sufficiently large that it cannot diffuse through the dialysis membrane.

## 5. CONCLUSIONS

A new DGT system, based on a liquid-binding layer containing a chitosan-stabilized gold nanoparticle suspension, was tested

for the colorimetric determination of nitrite—with partial success.

A chitosan-stabilized gold nanoparticle system was developed for the in situ determination of nitrite, which was quantitative over a large nitrite concentration range. An Fe(0)-p(AMPS/AMA) hydrogel used as the diffusion layer, for the reduction of nitrate to nitrite, was also developed. Nitrate rapidly reduced to nitrite, and the further reduction to  $\text{NH}_3/\text{NH}_4^+$  and  $\text{NO}_{x(g)}$  was avoided by the binding of nitrite to the binding layers. The diffusion characteristics were also determined. This work lays the foundations for the coupling of colorimetric techniques and DGT for the in-field quantitative determination of target species, such as nitrate; however, practical challenges remain.

Faster color reaction rates would improve the ability of the colorimetric nitrate DGT to provide quantitative nitrate concentrations, by better meeting the theoretical requirement of DGT for rapid and strong analyte binding to maintain the steady-state and concentration gradient.<sup>10</sup> Alternative binding layers to the AuNP-chitosan system could be pursued, conversely methods for increasing the reaction rate of the AuNP-chitosan system, which may be preferable, given the selectivity of the AuNP-chitosan system for nitrite. Removing the need for reduction of nitrate to nitrite for the colorimetric determination within the binding layer, by the development of a nitrate-selective AuNP, for example, would simplify the preparation of the DGT system. The development of a nitrate-selective rapid AuNP color reaction is difficult due to the unreactive nature of nitrate, but it would remove the need for the Fe(0)-p(AMPS/AMA) hydrogel. The Fe(0)-p(AMPS/AMA) hydrogel can be difficult to handle due the high degree of water swelling and relatively poor mechanical stability in comparison with the standard DGT APA hydrogels. Alternatively, incorporation of colorless or white reducing agents, such as nitrate reductase or Zn(0), into the liquid-binding layer would similarly overcome this. Successfully overcoming these limitations could result in an approach by which average nitrate concentrations in waterways could be measured in-field, that is likely usable by nonspecialists.

## ■ ASSOCIATED CONTENT

### SI Supporting Information

The Supporting Information is available free of charge at <https://pubs.acs.org/doi/10.1021/acsomega.1c06120>.

Synthesis and color reactions of the AuNP-rGO; FTIR, XRD, and SEM analyses of the gold nanoparticles and constituents and synthesis and SEM analysis of the Fe p(AMA/AMPS) hydrogel (PDF)

## ■ AUTHOR INFORMATION

### Corresponding Author

**Thomas D. W. Corbett** – *Environmental Research Institute, University of Waikato Faculty of Science and Engineering, The University of Waikato, Hamilton 3216, New Zealand*; Present Address: Geocentrum, Uppsala University, Villavägen 16, 752 36 Uppsala, Sweden; [orcid.org/0000-0001-6943-0373](https://orcid.org/0000-0001-6943-0373); Email: [corbett.tdw@gmail.com](mailto:corbett.tdw@gmail.com)

### Authors

**Adam Hartland** – *Environmental Research Institute, University of Waikato Faculty of Science and Engineering,*

*The University of Waikato, Hamilton 3216, New Zealand;*

[orcid.org/0000-0002-1864-5144](https://orcid.org/0000-0002-1864-5144)

**William Henderson** – *University of Waikato Faculty of Science and Engineering, The University of Waikato, Hamilton 3216, New Zealand*

**Gerald J. Rys** – *Ministry for Primary Industries, Wellington 6011, New Zealand*

**Louis A. Schipper** – *Environmental Research Institute, University of Waikato Faculty of Science and Engineering, The University of Waikato, Hamilton 3216, New Zealand*

Complete contact information is available at:

<https://pubs.acs.org/10.1021/acsomega.1c06120>

## Funding

DairyNZ and the New Zealand Ministry for Primary Industries funded this study.

## Notes

The authors declare no competing financial interest.

## ■ ACKNOWLEDGMENTS

We would like to acknowledge the financial support of DairyNZ and the Ministry for Primary Industries. We would also like to thank the late Professor Peter Teasdale for his guidance in moving toward liquid-binding layers, and a special thank you to Jacob Shrubsall and Peter Jarman for their help with 3D printing.

## ■ REFERENCES

- (1) Galloway, J. N.; et al. The Nitrogen Cascade. *BioScience* **2003**, *53*, 341–356.
- (2) Kissner, R.; Koppenol, W. H. Qualitative and Quantitative Determination of Nitrite and Nitrate with Ion Chromatography. *Methods Enzymol.* **2005**, *396*, 61–68.
- (3) Wang, Q.-H.; et al. Methods for the detection and determination of nitrite and nitrate: A review. *Talanta* **2017**, *165*, 709–720.
- (4) Nydahl, F. On the optimum conditions for the reduction of nitrate to nitrite by cadmium. *Talanta* **1976**, *23*, 349–357.
- (5) Śliwka-Kaszyńska, M.; Kot-Wasik, A.; Namieśnik, J. Preservation and Storage of Water Samples. *Crit. Rev. Environ. Sci. Technol.* **2003**, *33*, 31–44.
- (6) Audet, J.; et al. Comparison of sampling methodologies for nutrient monitoring in streams: uncertainties, costs and implications for mitigation. *Hydrol. Earth Syst. Sci.* **2014**, *18*, 4721–4731.
- (7) Maxwell, B. M.; et al. A small-volume multiplexed pumping system for automated, high-frequency water chemistry measurements in volume-limited applications. *Hydrol. Earth Syst. Sci.* **2018**, *22*, 5615–5628.
- (8) Zhang, H.; Davison, W. Performance Characteristics of Diffusion Gradients in Thin Films for the in Situ Measurement of Trace Metals in Aqueous Solution. *Anal. Chem.* **1995**, *67*, 3391–3400.
- (9) King, R. C.; Mulligan, P. K.; Stansfield, W. D. Diffusion. *A Dictionary of Genetics*, 8 ed.; Oxford University Press: Oxford, 2013; p 122.
- (10) Davison, W. *Diffusive Gradients in Thin-Films for Environmental Measurements*; Cambridge University Press: Cambridge, United Kingdom, 2016.
- (11) Ahmed, E. M. Hydrogel: Preparation, characterization, and applications: A review. *J. Adv. Res.* **2015**, *6*, 105–121.
- (12) Li, W.; et al. Application of a Poly(4-styrenesulfonate) Liquid Binding Layer for Measurement of  $\text{Cu}^{2+}$  and  $\text{Cd}^{2+}$  with the Diffusive Gradients in Thin-Films Technique. *Anal. Chem.* **2003**, *75*, 2578–2583.
- (13) Teasdale, P.; et al. Pore water sampling with sediment peepers. *TrAC, Trends Anal. Chem.* **1995**, *14*, 250–256.

- (14) Liu, S.; et al. A nanoparticulate liquid binding phase based DGT device for aquatic arsenic measurement. *Talanta* **2016**, *160*, 225–232.
- (15) Perez-Coronado, A. M.; et al. Selective Reduction of Nitrite to Nitrogen with Carbon-Supported Pd–AOT Nanoparticles. *Ind. Eng. Chem. Res.* **2017**, *56*, 11745–11754.
- (16) Ibrahim, M. H.; et al. Sensitive and selective colorimetric nitrite ion assay using silver nanoparticles easily synthesized and stabilized by AHNDMS and functionalized with PABA. *Nanoscale Adv.* **2019**, *1*, 1207–1214.
- (17) Amanulla, B.; et al. Selective Colorimetric Detection of Nitrite in Water using Chitosan Stabilized Gold Nanoparticles Decorated Reduced Graphene oxide. *Sci. Rep.* **2017**, *7*, 14182.
- (18) Lee, J. H.; et al. Highly sensitive and selective colorimetric sensors for uranyl (UO<sub>2</sub>(2+)): development and comparison of labeled and label-free DNAzyme-gold nanoparticle systems. *J. Am. Chem. Soc.* **2008**, *130*, 14217–14226.
- (19) Gunupuru, R.; et al. Colorimetric detection of Cu<sup>2+</sup> and Pb<sup>2+</sup> ions using calix[4]arene functionalized gold nanoparticles. *J. Chem. Sci.* **2014**, *126*, 627–635.
- (20) Zhang, Z.; et al. On-Site Visual Detection of Hydrogen Sulfide in Air Based on Enhancing the Stability of Gold Nanoparticles. *ACS Appl. Mater. Interfaces* **2014**, *6*, 6300–6307.
- (21) Sahiner, N.; et al. A soft hydrogel reactor for cobalt nanoparticle preparation and use in the reduction of nitrophenols. *Appl. Catal., B* **2010**, *101*, 137–143.
- (22) U.S. Environmental Protection Agency. *Method 350.1: Nitrogen, Ammonia (Colorimetric, Automated Phenate) Revision 2.0 edition*; Citeseer: Cincinnati, Ohio, 1993.
- (23) Ye, S.; Feng, J. The effect of sonication treatment of graphene oxide on the mechanical properties of the assembled films. *RSC Adv.* **2016**, *6*, 39681–39687.
- (24) Paredes, J. I.; et al. Graphene oxide dispersions in organic solvents. *Langmuir* **2008**, *24*, 10560–10564.
- (25) Khalil, I.; et al. Graphene-Gold Nanoparticles Hybrid-Synthesis, Functionalization, and Application in a Electrochemical and Surface-Enhanced Raman Scattering Biosensor. *Materials (Basel, Switzerland)* **2016**, *9*, 406.
- (26) Yan, N.; et al. Borate cross-linked graphene oxide–chitosan as robust and high gas barrier films. *Nanoscale* **2016**, *8*, 10783–10791.
- (27) Sutirman, Z. A.; et al. Preparation of methacrylamide-functionalized crosslinked chitosan by free radical polymerization for the removal of lead ions. *Carbohydr. Polym.* **2016**, *151*, 1091–1099.
- (28) Huang, J.; et al. Determining time-weighted average concentrations of nitrate and ammonium in freshwaters using DGT with ion exchange membrane-based binding layers. *Environ. Sci.: Processes Impacts* **2016**, *18*, 1530–1539.
- (29) Picioreanu, C.; van Loosdrecht, M. C. M.; Heijnen, J. J. Modelling the effect of oxygen concentration on nitrite accumulation in a biofilm airlift suspension reactor. *Water Sci. Technol.* **1997**, *36*, 147–156.
- (30) Corbett, T. D. W.; et al. Utility of Diffusive Gradients in Thin-Films for the measurement of nitrate removal performance of denitrifying bioreactors. *Sci. Total Environ.* **2020**, *718*, 135267.
- (31) Huang, J.; et al. Development and evaluation of the diffusive gradients in thin films technique for measuring nitrate in freshwaters. *Anal. Chim. Acta* **2016**, *923*, 74–81.
- (32) Emadi, F.; et al. Functionalized Graphene Oxide with Chitosan for Protein Nanocarriers to Protect against Enzymatic Cleavage and Retain Collagenase Activity. *Sci. Rep.* **2017**, *7*, 42258.
- (33) Ramasamy, R. P.; Maliyekkal, S. M. Formation of gold nanoparticles upon chitosan leading to formation and collapse of gels. *New J. Chem.* **2014**, *38*, 63–69.
- (34) Davison, W.; Zhang, H. Progress in understanding the use of diffusive gradients in thin films (DGT) – back to basics. *Environ. Chem.* **2012**, *9*, 1–13.
- (35) Kasaai, M. R.; Arul, J.; Charlet, G. Fragmentation of chitosan by ultrasonic irradiation. *Ultrason. Sonochem.* **2008**, *15*, 1001–1008.
- (36) Davison, W.; et al. Distribution of dissolved iron in sediment pore waters at submillimetre resolution. *Nature* **1991**, *352*, 323–325.
- (37) Pigaleva, M. A.; et al. Stabilization of Chitosan Aggregates at the Nanoscale in Solutions in Carbonic Acid. *Macromolecules* **2014**, *47*, 5749–5758.
- (38) Uher, E.; et al. Impact of Biofouling on Diffusive Gradient in Thin Film Measurements in Water. *Anal. Chem.* **2012**, *84*, 3111–3118.
- (39) Sogias, I. A.; Khutoryanskiy, V. V.; Williams, A. C. Exploring the Factors Affecting the Solubility of Chitosan in Water. *Macromol. Chem. Phys.* **2010**, *211*, 426–433.



ACS  
**MEASUREMENT  
SCIENCE** Au  
AN OPEN ACCESS JOURNAL OF THE AMERICAN CHEMICAL SOCIETY

 Editor-in-Chief  
**Prof. Shelley D. Minteer**  
University of Utah, USA

**Open for Submissions** 

pubs.acs.org/measureau  ACS Publications  
Most Trusted. Most Cited. Most Read.